

3635

Optimization of B_0 Simulation Strategy in the Human Heart based on CT Images at limited Field of View

Yun Shang¹, Sebastian Theilenberg¹, Laura M. Schreiber^{2,3}, and Christoph Juchem^{1,4}¹Department of Biomedical Engineering, Columbia University, New York, NY, United States, ²Chair of Cellular and Molecular Imaging, Comprehensive Heart Failure Center, University Hospital Wuerzburg, Wuerzburg, Germany, ³Department of Cardiovascular Imaging, Comprehensive Heart Failure Center, University Hospital Wuerzburg, Wuerzburg, Germany, ⁴Department of Radiology, Columbia University Medical Center, New York, NY, United States

Synopsis

B_0 simulation in the heart based on thoracic CT images is a powerful tool to investigate cardiac B_0 conditions in the general population for the development of an optimized cardiac B_0 shimming strategy. Thoracic CT scans typically have a limited field of view posing a challenge to the accuracy of field simulations. Here we present a systematic analysis of errors introduced by B_0 computations in the human heart from CT-based susceptibility distributions of limited field of view and present strategies to resemble B_0 conditions in the human heart to achieve elevated accuracy with model-based addition of selected anatomical features.

Introduction

Human cardiac MRI adopting balanced steady-state free precession (SSFP) sequences suffers from dark band artifacts¹ due to B_0 inhomogeneity^{2,3}. The best remedy for mitigating this issue is to homogenize B_0 distribution in the heart through B_0 shimming⁴. The development of an optimized cardiac B_0 shimming strategy in the general population necessitates understanding B_0 conditions encountered in the human heart. We recently presented proof-of-principle for efficiently obtaining cardiac B_0 maps by field simulation based on susceptibility distributions derived from readily available whole-thoracic CT images⁵. However, thoracic CT scans typically have a limited Field of View (FOV) that does not include the entire body's susceptibility information, causing a challenge to field simulation accuracy due to 1) boundary effects potentially stretching across the entire FOV when using rapid FFT-based numerical methods⁶⁻⁸ and 2) lack of relevant anatomical structures contributing to B_0 conditions in the heart such as head, shoulders, arms, and legs (Figure 1). Here, we present a systematic analysis of errors induced by B_0 simulation in the heart from CT-based susceptibility distributions of limited FOV and strategies to achieve elevated accuracy with model-based addition of selected anatomical features.

Methods

The fidelity of B_0 field simulations in the human heart was analyzed employing two numerical models, "Duke" and "Ella"⁹ (Virtual Population V2.0 models, IT'IS Foundation, Zurich, Switzerland). A gold standard was established by computing B_0 distributions as the superposition of dipole fields¹⁰ for the entire body, i.e., from head to toe. B_0 simulations utilizing the FFT-based method and under specific conditions, e.g., limited FOV, were then compared to this gold standard. The simulation error was characterized as the standard deviation (STD) of field differences between the two methods in the heart. The effects induced by the discretization of susceptibility distributions and boundary effects of finite computation volume⁸ were investigated individually by calculating B_0 maps at different spatial resolutions (2 mm through 9 mm isotropic) and zero-padding factors (1.5 to 6.0) to find the best possible accuracy while maintaining a matrix size that can be handled computationally (Dell Poweredge T440, CPU: Intel Xeon 4116, RAM: 64 GB). Field calculations were performed for 3 T using B0DETOX¹¹ software.

To mitigate the effects on B_0 distribution in the heart caused by lack of anatomical structures, we investigated adopting anatomical parts from another generic body. Model Duke was cut to the FOV of a typical thoracic CT scan and extended from model Ella by adopting head, including shoulder (type 1), legs (type 2) and arms (type 3) step by step. Replacing the legs by repeating the last body slice instead of zero-filling was further investigated for types 2 and 3 to reduce matrix size, leading to types 4 and 5 (Figure 3A). The performance of these extension approaches in FFT-based field simulations were evaluated by analyzing the B_0 field differences compared to the simulation using Duke's entire body.

We further tested the performance of types 3 (all anatomical parts) and 4 (minimum matrix size) by applying them to 10 male and 10 female human models¹² with various BMIs. We investigated the strategies 1) adopting parts from Duke to male models and Ella to female models and 2) extending models from another body with similar BMI by field comparison to each model's entire body at 2.5 mm isotropic. The simulation error of type 4 at the highest achievable resolution (1 mm isotropic) was estimated by scaling the STD by a factor extrapolated from the simulation data.

Results

The standard deviation of the field differences between the FFT-based and dipole method decreased with improved zero-padding factor then converged at a factor between 2 and 3, beyond which spatial resolution has a more prominent effect on the simulation accuracy (Figure 2). The higher spatial resolution led to more accurate results with smaller STD values for all zero-padding factors. Therefore, we chose a zero-padding factor of 2.5 and the highest possible spatial resolution of 2 mm isotropic within the computation capability.

All anatomical extension approaches showed substantially less B_0 simulation errors than the original CT-type FOV with more homogeneous field differences and lower STD values (Figure 3B and 4). The anatomical extension type 3 adopting the body with a similar BMI exhibited the lowest B_0 simulation error with an average STD of 1.2 Hz across female models and 1.1 Hz in male models (Figure 5). The STD values of type 4 at 1 mm resolution with similar BMI, scaled by a factor of 0.78, was more comparable to type 3. Type 4 was a suitable compromise to achieve high-resolution B_0 simulation with less discretization error under limited computation power.

Discussion

Here we present an analysis of the impact of spatial resolution, zero-padding factor, and anatomical extension on cardiac B_0 simulation accuracy at 3 T. We disentangled and quantified error sources associated with cardiac B_0 distributions when computed from magnetic susceptibility distributions of limited FOV. We demonstrated that high B_0 fidelity can be achieved with the model-based extension of human anatomy on a regular PC. The derived simulation approach will be used to compute cardiac B_0 maps from a large set of CT images for the development of a population-based cardiac B_0 shimming strategy.

Acknowledgements

No acknowledgement found.

References

1. Ferreira PF, Gatehouse PD, Mohiaddin RH, Firmin DN. Cardiovascular magnetic resonance artefacts. *J Cardiovasc Magn Reson*. 2013;15(1):41.
2. Atalay MK, Poncelet BP, Kantor HL, Brady TJ, Weisskoff RM. Cardiac susceptibility artifacts arising from the heart-lung interface. *Magn Reson Med*. 2001;45(2):341-345.
3. Schär M, Kozerke S, Fischer SE, Boesiger P. Cardiac SSFP imaging at 3 Tesla. *Magn Reson Med*. 2004;51(4):799-806.
4. Juchem C, de Graaf RA. B_0 magnetic field homogeneity and shimming for in vivo magnetic resonance spectroscopy. *Analytical Biochemistry*. 2017;529:17-29.

5. Shang Y, Theilenberg S, Mattar W, Terekhov M, Jambawalikar SR, Schreiber L, Juchem C. High Resolution Simulation of B₀ Field Conditions in the Human Heart Based on Segmented CT Images. Proc Int Soc Magn Reson Med 2019;2184.
6. Marques J, Bowtell R. Application of a Fourier-based method for rapid calculation of field inhomogeneity due to spatial variation of magnetic susceptibility. Concepts Magn Reson. 2005;25B(1):65-78.
7. Salomir R, de Senneville BD, Moonen CT. A fast calculation method for magnetic field inhomogeneity due to an arbitrary distribution of bulk susceptibility. Concepts Magn Reson. 2003;19B(1):26-34.
8. Koch KM, Papademetris X, Rothman DL, de Graaf RA. Rapid calculations of susceptibility-induced magnetostatic field perturbations for in vivo magnetic resonance. Phys Med Biol. 2006;51(24):6381-6402.
9. Gosselin MC, Neufeld E, Moser H, Huber E, Farcito S, Gerber L, Jedensjo M, Hilber I, Di Gennaro F, Lloyd B, Cherubini E, Szczerba D, Kainz W, Kuster N. Development of a new generation of high-resolution anatomical models for medical device evaluation: the Virtual Population 3.0. Phys Med Biol. 2014;59(18):5287-5303.
10. Muller-Bierl B, Graf H, Steidle G, Schick F. Compensation of magnetic field distortions from paramagnetic instruments by added diamagnetic material: measurements and numerical simulations. Med Phys. 2005;32(1):76-84.
11. Juchem C. B0DETOX - B₀ Detoxification Software for Magnetic Field Shimming. Columbia TechVenture (CTV), License CU17326 2017; innovation.columbia.edu/technologies/cu17326_b0detox
12. Segars WP, Sturgeon G, Mendonca S, Grimes J, Tsui BM. 4D XCAT phantom for multimodality imaging research. Med Phys. 2010;37(9):4902-4915.

Figures

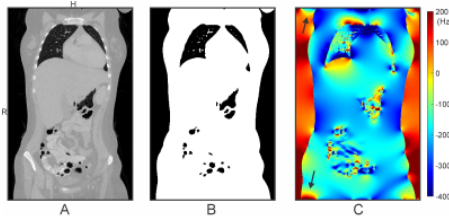


Figure 1. The procedure of B₀ simulation in the human heart based on whole thoracic CT images. A) Exemplary whole thoracic CT image of one subject and B) derived susceptibility distribution with magnetic susceptibility of -9 ppm and 0 ppm assigned for human tissue (white) and air cavity (Black)⁵. C) B₀ field distribution inside the body was simulated based on the rapid FFT method⁶⁻⁸. Obvious field artifacts (arrows) were observed at the boundary of the limited FOV, and it might also include artifacts that can be hard to spot. The B₀ simulation accuracy in the heart is quantified in this work.

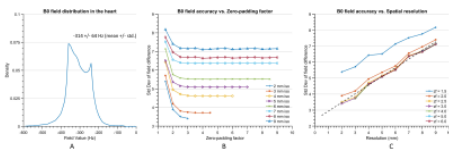


Figure 2. Comparison of simulated B₀ fields in the heart between the FFT-based method and dipole method. A) Exemplary field distribution in the heart was calculated using dipole method based on the susceptibility distribution of Ella's entire body at 3 mm isotropic. The standard deviation of the field difference was shown B) from fine to coarse resolution and C) a range of zero-padding factors. Zero-padding factors higher than 2.5 do not substantially improve the STD value, i.e., B₀ accuracy, while a higher resolution can significantly lower this value (dash line: linear fit at $z_f = 2.5$).

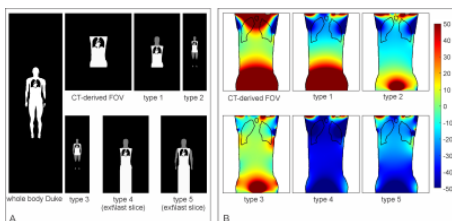


Figure 3. A) Susceptibility distribution of Duke's entire body and different anatomical extension types of CT-derived FOV of model Duke (White) with anatomical parts from model Ella (Grey). The computation volume was extended along x, y, and z with zero-padding (Black) using a factor of 2.5. B) The simulated B₀ field difference between anatomical extensions and Duke's entire body, adopting the FFT-based method at a spatial resolution of 2 mm isotropic, indicates the influence of the anatomical structure to the B₀ field distribution in the heart beyond the CT-derived FOV.

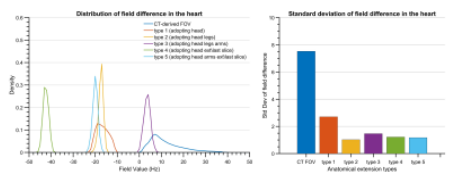


Figure 4. Histogram distribution (left) and standard deviation (right) of the field difference in the heart between susceptibility distribution after anatomical extension and Duke's entire body (refer to Figure 3B). The B₀ simulation error with anatomical extensions was at least three times less than the susceptibility distribution of CT-derived FOV. The extension type with legs (types 2/3) or repeating the last body slice (types 4/5) reduced the STD more than only adding the head (type 1) which indicates the necessity of extending along foot direction for elevating field accuracy.

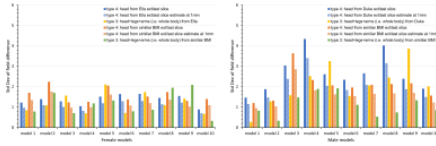


Figure 5. The standard deviation of field difference between the extended CT-derived FOV and the entire body for ten female models (left) and ten male models (right). The anatomical extension type 3 adopting the body with a similar BMI exhibited the lowest B_0 simulation error compared to other types, especially in male models. It is the optimized strategy when sufficient computation power is available while simplified anatomical extension type 4 are reasonable compromises to achieve high-resolution B_0 simulation with less discretization error under limited computation resources.